Current Biology

Article

Associative learning in the box jellyfish *Tripedalia cystophora*

Graphical abstract

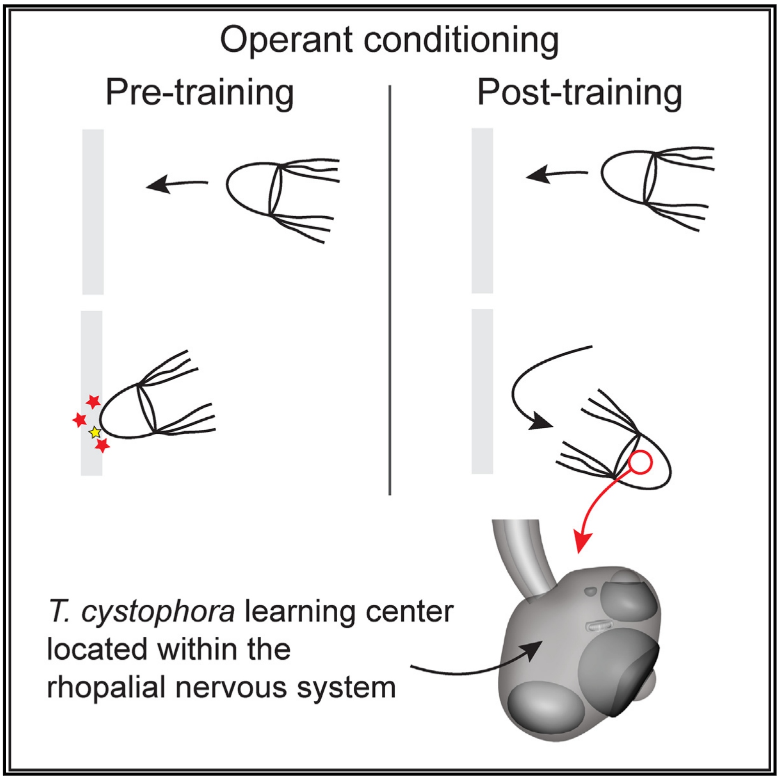
Operant conditioning
Pre-training
Post-training
T. cystophora learning center located within the rhopalial nervous system

Highlights

- The box jellyfish *Tripedalia cystophora* is capable of associative learning
- Learning is based on the combination of visual and mechanical stimuli
- The rhopalial nervous system (RNS) is the learning center of *Tripedalia cystophora*

Authors

Jan Bielecki, Sofie Katrine Dam Nielsen, Gösta Nachman, Anders Garm

Correspondence

jan@bielecki.dk (J.B.),
algarm@bio.ku.dk (A.G.)

In brief

Bielecki et al. show that *Tripedalia cystophora* is capable of associative learning by combining visual and mechanosensory stimuli and that learning resides within the rhopalial nervous system (RNS). It is the first time that associative learning has been verified at such a basic evolutionary level.

Bielecki et al., 2023, Current Biology *33*, 1–10
October 9, 2023 © 2023 Elsevier Inc.
https://doi.org/10.1016/j.cub.2023.08.056

CellPress

Please cite this article in press as: Bielecki et al., Associative learning in the box jellyfish *Tripedalia cystophora*, Current Biology (2023), https://doi.org/10.1016/j.cub.2023.08.056

Current Biology

CellPress

Article

Associative learning in the box jellyfish *Tripedalia cystophora*

Jan Bielecki,[1,4,5,*] Sofie Katrine Dam Nielsen,[2] Gösta Nachman,[3] and Anders Garm[2,4,*]
[1]Institute of Physiology, Kiel University, 24118 Kiel, Germany
[2]Marine Biological Section, University of Copenhagen, 2100 Copenhagen, Denmark
[3]Section of Ecology and Evolution, University of Copenhagen, 2100 Copenhagen, Denmark
[4]These authors contributed equally
[5]Lead contact
*Correspondence: jan@bielecki.dk (J.B.), algarm@bio.ku.dk (A.G.)
https://doi.org/10.1016/j.cub.2023.08.056

SUMMARY

Associative learning, such as classical or operant conditioning, has never been unequivocally associated with animals outside bilatarians, e.g., vertebrates, arthropods, or mollusks. Learning modulates behavior and is imperative for survival in the vast majority of animals. Obstacle avoidance is one of several visually guided behaviors in the box jellyfish, *Tripedalia cystophora* Conant, 1897 (Cnidaria: Cubozoa), and it is intimately associated with foraging between prop roots in their mangrove habitat. The obstacle avoidance behavior (OAB) is a species-specific defense reaction (SSDR) for *T. cystophora*, so identifying such SSDR is essential for testing the learning capacity of a given animal. Using the OAB, we show that box jellyfish performed associative learning (operant conditioning). We found that the rhopalial nervous system is the learning center and that *T. cystophora* combines visual and mechanical stimuli during operant conditioning. Since *T. cystophora* has a dispersed central nervous system lacking a conventional centralized brain, our work challenges the notion that associative learning requires complex neuronal circuitry. Moreover, since Cnidaria is the sister group to Bilateria, it suggests the intriguing possibility that advanced neuronal processes, like operant conditioning, are a fundamental property of all nervous systems.

INTRODUCTION

An impressive diversity of behaviors can be observed across the Metazoa, from slowly pulsing jellyfish to dancing peacock spiders and socially grooming primates. This diversity is not only prominent on an interspecies level but also on an intra-species and even individual level—individual animals respond differently to the same sensory stimulus at different times. Plasticity in the behavioral repertoire is a distinguishing characteristic of all examined animals and vital to their evolutionary success in general.[1] Several mechanisms can shape behavioral plasticity, but the influence of previous experience—memory formation and learning—is undoubtedly among the most important.

Learning in general spans a wide range of complexities from simple sensitization and habituation to highly advanced learning such as insight and reasoning.[2] Memory formation and learning in animals reside within the nervous system, with the general notion that more advanced nervous systems accomplish more advanced types of learning.[2] Due to the immense neural network complexity of most animal brains (even the *Drosophila melanogaster* brain comprises approximately 200,000 neurons and millions of synapses[3]), several aspects of the neurobiology of learning are still enigmatic.[4] While classical work on the gastropod *Aplysia californica* provided detailed understanding of simple habituation and sensitization,[5] much less is known about the cellular mechanisms of more advanced types of learning. Consequently, a better understanding at the systems level requires a more tractable model system that performs associative learning within much smaller and simpler neuronal circuitry, such as the nematode *Caenorhabditis elegans*.[6]

Cnidarians are among the simplest animals with a nervous system, and they have mostly been found to display non-associative learning, such as sensitization and habituation.[7,8] In the past, merely three studies have addressed associative learning in cnidarians, all using sea anemones,[9–12] but the interpretation of their results is not straightforward (discussed later). All three studies emphasize the need to identify a pliable model organism with distinct behaviors.

Within cnidarians, box jellyfish are extraordinary in behavioral complexity. In particular, the Caribbean box jellyfish *Tripedalia cystophora* (Figure 1A) displays mating behavior with internal fertilization and is, owing to its image-forming eyes, capable of visually guided navigation and obstacle avoidance.[13–17] Not only do the relatively simple *T. cystophora* nervous system and the dominating visual sensory modality offer a unique advantage as a model system for associative learning, but Cnidaria being a basal phylum in nervous system evolution also holds a key position for understanding basic neuronal function. Like other cnidarians, *T. cystophora* does not possess a single centralized brain but has instead a concentration of neurons in the four eye-bearing sensory structures (rhopalia, Figure 1B), which serve as individual visual processing and integration centers. In the

© 2023 Elsevier Inc.

Please cite this article in press as: Bielecki et al., Associative learning in the box jellyfish *Tripedalia cystophora*, Current Biology (2023), https://doi.org/10.1016/j.cub.2023.08.056

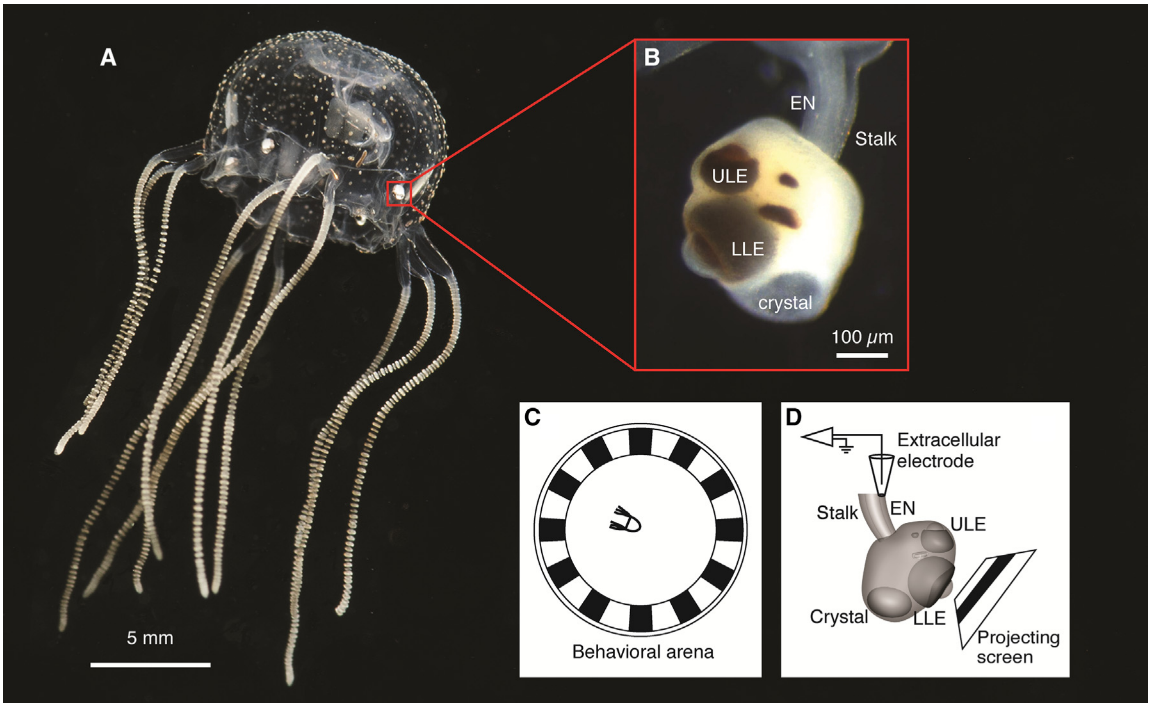

Figure 1. Behavioral and neurophysiological training regimes for associative learning in the box jellyfish *Tripedalia cystophora*

(A) Adult specimen of the box jellyfish *T. cystophora*.

(B) The visual system of the box jellyfish is located on four sensory structures (rhopalia) and includes two lens eyes, the upper and lower lens eye (ULE and LLE), structurally similar to vertebrate eyes. Each rhopalium also contains a visual information processing center.

(C) In the behavioral arena the "obstacles" on the perimeter wall mimic the prop roots in the mangrove habitat of *T. cystophora*. Using this setup, we tested how the jellyfish responded to obstacles of different contrast and demonstrated that they learn to avoid low-contrast obstacles by combining visual and mechanical stimuli during unsuccessful avoidances.

(D) In the neurophysiological setup, moving obstacles were presented directly to the LLE of an isolated rhopalium. The corresponding pacemaker signals (recorded from the epidermal stalk nerve EN) reflect the swimming behavior of *T. cystophora*. Here, the animals learn to avoid low-contrast obstacles through classical conditioning using weak electrical pulses.

adult medusa, these rhopalial nervous systems (RNSs) comprise merely about one thousand processing neurons each.[18] Central to the RNS is a dense neuropil with tiny neurites, as small as 100 nm in diameter, and a high number of both uni- and bidirectional synapses.[18] The RNS comprises several subsystems, as indicated by the differential application of neurotransmitters including several neuropeptides, and some of these subsystems form connections between the six eyes of the rhopalium.[19,20] In the proximal end of the rhopalium, a cluster of giant neurons have been identified as the putative swim pacemakers of the jellyfish, which control the swim pulses in a 1:1 manner.[21] The swim pacemaker frequency is strongly influenced by the visual input to the rhopalium.[22]

The behavioral repertoire of *T. cystophora* is intimately connected to their mangrove lagoon habitat where the jellyfish forage on copepod prey found between prop roots of the *Rhizophora mangle* trees growing at the edge of the lagoon.[23,24] Particularly important for the medusa is to avoid damage to their fragile body, which happens through collisions with the prop roots. The medusae of *T. cystophora* thus display a visually guided obstacle avoidance behavior (OAB) mediated by the lower lens eye (LLE).[13] The OAB is characterized by an increased swim pacemaker activity leading to rapid pulsing and 120°–180° turning away from the obstacle.[13] Performing the OAB at the right time and distance to the object is of critical importance—too late results in frequent collisions, and too soon interferes with optimal foraging behavior.[23] To correctly time the OAB, *T. cystophora* evaluates the distance to obstacles using the visual contrast between object and surrounding water.[25]

Optimal performance of OAB is further complicated in their mangrove habitat, however, since the relationship between contrast and distance (contrast:distance) is far from constant and varies dramatically with changes in water turbidity. The turbidity changes frequently, often hourly, due to tide, rainfall, waves, and dynamic algal communities, affecting the concentration and types of suspended particles, which scatter and absorb the light.[26] As such, a mid-contrast object means safe distance in clear water but close to collision in turbid water, and it is therefore critical for *T. cystophora* to calibrate contrast:distance accordingly to optimize OAB and time spent foraging. At night, when the activity of *T. cystophora* diminishes and the animal presumably attaches to sea grass or seaweed, OAB becomes irrelevant.[27]

In order to test the hypothesis that *T. cystophora* is capable of calibrating contrast:distance through learning processes based on a combination of visual and mechanical stimuli during unsuccessful OAB events (i.e., collisions), we conducted a series of behavioral (Figure 1C) and *ex vivo* neurophysiological experiments (Figure 1D) in which individuals were exposed to visual

Please cite this article in press as: Bielecki et al., Associative learning in the box jellyfish *Tripedalia cystophora*, Current Biology (2023), https://doi.org/10.1016/j.cub.2023.08.056

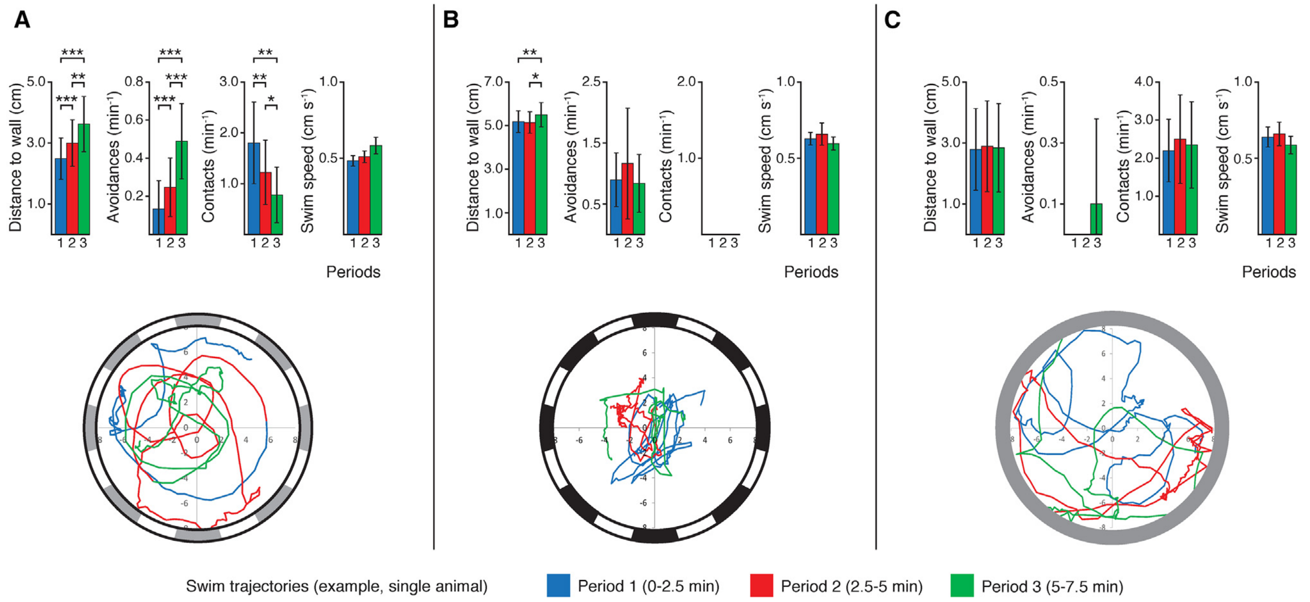

Figure 2. Behavioral evidence of associative learning, operant conditioning, in the box jellyfish *Tripedalia cystophora*

(A) When presented with gray obstacles of a contrast below initial response threshold ($c = 0.39$), the jellyfish initially swam along the arena wall as seen by the trajectory. This provided both visual (gray obstacles) and mechanical (wall contacts) stimuli. Within the 7.5 min trial period, the jellyfish learned to significantly increase the distance to the arena wall and the frequency of avoidances. Importantly, they also more than halved their contacts with the wall. These results suggest associative learning (operant conditioning) in *T. cystophora* by combining visual and mechanical stimuli.

(B) Presenting the naive jellyfish with high-contrast black obstacles ($c = 0.93$) centered them in the behavioral arena and resulted in a complete lack of collisions with the perimeter wall throughout the trial period. Furthermore, this lack of mechanical aversive stimulation resulted in a constant frequency of avoidances but also in a small (~6%), though significant, increase in the average distance to the obstacles. These results show that learning did not take place with visual stimulation alone.

(C) In the experiments without visual contrast (uniform gray wall), the jellyfish in general failed to perform avoidances and spent most of the time swimming along the arena wall with a high frequency of collisions. This setup with only the aversive mechanical stimulation did not lead to learning, as seen by the lack of significant changes in any of the observed behavioral parameters. Note that for all three visual scenarios the medusae kept the same average swim speed (activity level) through the three periods (Period 1: 0–2.5 min, Period 2: 2.5–5 min, and Period 3: 5–7.5 min; Tables 1 and 2). Asterisks denote levels of significance (*$p < 0.05$, **$p < 0.001$, and ***$p < 0.0001$). Error bars ±SE.

and/or mechanical stimulation. Evidence of associative learning (classical and operant conditioning) requires that the individuals improve their OAB performance after being presented to both types of stimuli simulaneously, but not when one of the stimuli is absent.

RESULTS

Behavioral experiments

We used four measures to quantify the behavior of *T. cystophora* medusae: (1) average distance to the obstacles (arena wall), (2) frequency of successful obstacle avoidances, (3) frequency of unsuccessful obstacle avoidances (wall contacts), and (4) the average swim speed. An avoidance response was defined as the medusa swimming toward the wall and then turning a minimum of 120° in two or three swim contractions with an increased pulse rate (see Garm et al. [2013][25] for a supplementary video of this behavior). An unsuccessful avoidance was defined as a contact between the bell of the medusa and the arena wall. Throughout the experiments the medusae stayed in the upper part of the water column without touching the floor of the arena.

When *T. cystophora* was presented with obstacles at a contrast below the initial response threshold ($c = 0.39$) on the perimeter wall of the behavioral arena (see STAR Methods), the animals initially collided with the wall (Figure 2A). With continued exposure to low-contrast obstacles, the medusae, through unsuccessful obstacle avoidances, learned to significantly ($\chi^2_2 = 8.65$; $p < 0.0001$) increase the average distance to the wall by approximately 50% during the 7.5 min trial (2.48 ± 0.20 cm in the initial 2.5 min to 3.62 ± 0.26 cm in the last 2.5 min, $\bar{x}$ ± SE). In the same period, the number of successful OABs also increased significantly ($\chi^2_2 = 8.53$; $p < 0.0001$), namely almost quadrupling from 0.13 ± 0.04 to 0.49 ± 0.06, no. of avoidances (min^{-1}) $\bar{x}$ ± SE. Most importantly, within the 7.5 min trial period the animals had significantly adjusted their contrast:distance response ($\chi^2_2 = 6.16$; $p = 0.0017$) to less than half the number of contacts with the perimeter wall (1.80 ± 0.23 to 0.78 ± 0.16, no. of contacts [min^{-1}] $\bar{x}$ ± SE) (Figure 2A and Tables 1 and 2). These findings strongly suggest operant conditioning in the box jellyfish *T. cystophora* as they seemingly learn the positive/negative consequences of their behavior.[1]

According to our hypothesis, both visual and mechanical stimuli are needed to induce learning. We tested this hypothesis by means of experiments presenting the two types of stimuli separately. In "visual stimulation only" trials, where the medusae were exposed to high-contrast obstacles ($c = 0.93$), *T. cystophora* individuals

Table 1. Differences between behavior of *Tripedalia cystophora* exposed to different visual stimuli

		Distance			Avoidance			Contacts			Swim speed		
Effect	df	MS	*F*	p	MS	*F*	p	MS	*F*	p	MS	*F*	p
ID	24	2.490	12.14	**<0.0001**	0.844	3.17	**0.0003**	1.771	3.35	**0.0002**	0.052	3.18	**0.0003**
Treatment	2	41.944	*16.84*	**<0.0001**	32.93	*39.0*	**<0.0001**	95.94	*54.2*	**<0.0001**	0.106	*2.05*	0.1501
Period	2	1.650	8.04	**0.0010**	1.376	5.16	**0.0093**	1.782	3.38	**0.0425**	0.005	0.29	0.7522
Treatment*period	4	0.845	4.12	**0.0060**	1.089	4.09	**0.0063**	1.712	3.24	**0.0196**	0.023	1.41	0.2465
Error	48	0.205			0.266			0.528			0.016		

Results of manovas (multivariate analysis of variance) testing for an overall effect of *ID*, *Treatment*, and *Period* on *Distance*, *Avoidance*, *Contacts*, and *Swim speed* in the behavioral trials. df = degrees of freedom; MS = mean squared deviations (i.e., MS = SS/df, where SS = sum of squared deviations). The overall effects of *Treatment* (i.e., stimulus type) and *Period* (i.e., effect of learning) were significant (Wilk's λ for *Treatment* = 0.0212, $F_{8,90} = 66.03$, $p < 0.0001$; Wilk's λ for *Period* = 0.611, $F_{8,90} = 3.14$, p = 0.0035). Values in italics: *F* for *Treatment* was obtained as $F_{2,24}$ = MS(*Treatment*)/MS(*ID*), because *ID* is a random factor. Significant values ($p < 0.05$) are shown in bold.

were never close enough to the perimeter wall to collide, resulting in an absence of mechanical input (Figure 2B). Accordingly, the frequency of OABs did not change significantly ($\chi^2_2 = 0.41$; p = 0.93) over time (0.90 ± 0.17 to 0.84 ± 0.18, no. of avoidances [min^{-1}] $\bar{x}$ ± SE), while the average distance to the perimeter wall increased slightly (5.18 ± 0.20 to 5.50 ± 0.22, distance [cm] $\bar{x}$ ± SE), though significantly ($\chi^2_2 = 5.10$; p = 0.0012) within the 7.5 min trial (Tables 1 and 2). Likewise, in experiments where the animals were exposed to a uniform gray perimeter wall (luminance matching the average luminance in the high-contrast arena), they continued to collide with the wall (Figure 2C). However, since mechanical input was disconnected from visual input, learning did not occur, as revealed by the constancy of the test parameters, distance to wall ($\chi^2_2 = 0.14$; p = 0.98), avoidance rate ($\chi^2_2 = 1.0$; p = 0.53), and contacts with the wall ($\chi^2_2 = 1.15$; p = 0.97) (Tables 1 and 2). The average swim speed of the medusae remained approximately constant throughout the trials for all three visual scenarios (gray stripes: $\chi^2_2 = 2.08$; $p > 0.25$, black stripes: $\chi^2_2 = 3.17$; $p > 0.31$, uniform gray: $\chi^2_2 = 1.12$; $p > 0.51$), which indicates that the changes in the three other behavioral parameters after exposure to gray stripes were not just caused by the animals being less active.

Neurophysiological experiments

Since an OAB is characterized by a rapid increase in swim contractions, resulting in burst swimming, the signal frequencies of the swim pacemaker can be used as proxy for avoidance behavior. Swim pacemaker signals are generated in the RNS and can be recorded from the efferent epidermal stalk nerve of the rhopalium.[21,28] This offers the advantage of experimenting on an isolated rhopalium positioned to face a projecting screen, thereby providing complete control of the images presented to the LLE (Figure 1D). Since successful learning of the contrast:distance in *T. cystophora* may require not only visual stimuli but also concurrent mechanical stimuli, using isolated rhopalia poses the experimental challenge of having severed the neuronal connection to the mechanosensory apparatus of the bell. We reason that an electrical stimulation will reach the pacemaker cell clusters as a mechanosensory mimic when applied to the suction electrode that records the swim pacemaker signals from the bidirectional epidermal stalk nerve.[29] Mechanosensory stimulation was therefore presented to the RNS as a weak electrical pulse, analogous to operant training in *Aplysia*[30] and rodents (e.g., Reynolds et al.[31]) (see STAR Methods for details). The classical training protocol employed a moving bar with contrast *c* = 0.20 as the conditioned stimulus (CS) and a weak electrical pulse (100 mV at 100 nA for 50 ms) as the unconditioned stimulus (US). We performed pre- and post-training analyses of behavioral responses to moving obstacles with three levels of contrasts (*c* = 0.20, 0.40, and 0.80) and used a three-parameter model (see STAR Methods) to reveal whether a stimulation of the RNS caused a significant increase in spike activity (measured as the peak value, y_m), interpreted as an OAB response.

Training significantly increased pacemaker responsiveness to all levels of contrast (*c* = 0.20, 0.40, and 0.80) when the RNS was exposed to concurrent visual and mechanosensory stimuli (CS and US). Conversely, training did not significantly affect responsiveness to any contrast levels in treatments where visual and mechanical stimulation were administered separately or temporally uncoupled (unpaired) (Figure 3; Tables 3 and 4).

In the pre-training trials, the RNS was only responsive to the high-contrast (*c* = 0.80) visual stimulation (y_m ± SE: 1.32 ± 0.10, 0.93 ± 0.14, 1.21 ± 0.12, and 1.55 ± 0.17 in the "CS + US," "CS only," "US only," and "unpaired CS + US" pre-training phases, respectively, Figure 3). In the pre-training trials, the rhopalia showed no response to contrast levels *c* = 0.20 (model did not converge, implying no reaction, in the "CS + US," "CS only," and "US only" pre-training phases, and y_m ± SE: 0.86 ± 0.48 in "unpaired CS + US") and *c* = 0.40 (y_m ± SE: 0.11 ± 0.08, 0.22 ± 0.08, 1.05 ± 0.44, and 0.40 ± 0.21 in the "CS + US," "CS only," "US only," and "unpaired CS + US" pre-training phases, respectively) (Figure 3; Table 3).

In the post-training phase, the RNS further responded to low-contrast *c* = 0.20 (y_m ± SE: 0.29 ± 0.06) and mid-contrast *c* = 0.40 (y_m ± SE: 0.96 ± 0.12), and it responded significantly more to high-contrast *c* = 0.80 visual stimulation than in the pre-training phase (y_m ± SE: 1.32 ± 0.10 vs. 1.53 ± 0.10 in the pre- and post-training phases, respectively) (Figures 3A and S1; Table 3 and 4). When a significant OAB response occurred, it peaked after 6–7 s, which is slightly before the leading edge of the bar reached the center of the visual field. The peak occurred earlier with increasing contrast (Figures S1–S4; Table 3).

DISCUSSION

Previous work has convincingly demonstrated non-associative types of learning in cnidarians, such as sensitization and

Table 2. Changes in behavior of *Tripedalia cystophora* caused by different visual stimuli

			Period 1 0–2.5 min		Period 2 2.5–5 min		Period 3 5–7.5 min		ANOVA				Turkey's HSD post-hoc test		
Treatment	Parameters	*N*	$\bar{x}$	SE	$\bar{x}$	SE	$\bar{x}$	SE	Effect	df	X^2	p	P1 vs. P2	P2 vs. P3	P1 vs. P3
Gray obstacles *c* = 0.39	Distance	12	2.485	0.199	2.997	0.223	3.620	0.264	ID	11	10.44	0.4914			
									period	2	8.65	**0.0132**	**0.0007**	**0.0062**	**<0.0001**
	Avoidance	12	0.133	0.043	0.278	0.045	0.489	0.058	ID	11	11.88	0.3730			
									period	2	8.53	**0.0140**	**0.0001**	**0.0002**	**<0.0001**
	Contacts	12	1.800	0.234	1.222	0.185	0.778	0.160	ID	11	11.16	0.4296			
									period	2	6.16	**0.0459**	**0.0064**	**0.0232**	**0.0017**
	Swim speed	12	0.483	0.036	0.509	0.040	0.583	0.057	ID	11	11.00	0.4430			
									period	2	2.08	0.3527	0.8551	0.4852	0.2509
Black obstacles *c* = 0.93	Distance	7	5.176	0.193	5.137	0.192	5.496	0.218	ID	6	6.85	0.3350			
									period	2	5.1	0.0779	0.9639	**0.0147**	**0.0012**
	Avoidance	7	0.895	0.169	1.162	0.345	0.838	0.181	ID	6	6.12	0.4100			
									period	2	0.41	0.8165	0.9096	0.7904	0.9257
	Contacts	7	0	0	0	0	0	0	ID	6	0	1			
									period	2	0	1	1	1	1
	Swim speed	7	0.628	0.044	0.658	0.075	0.596	0.045	ID	6	5.12	0.5291			
									period	2	3.17	0.2041	0.8561	0.3137	0.4381
Uniform gray	Distance	8	2.785	0.479	2.889	0.531	2.839	0.515	ID	7	6.75	0.4550			
									period	2	0.14	0.9320	0.9433	0.9326	0.9756
	Avoidance	8	0	0	0	0	0.100	0.100	ID	7	1.30	0.9884			
									period	2	1.00	0.3173	1	0.5333	0.5333
	Contacts	8	2.200	0.203	2.500	0.412	2.350	0.403	ID	7	8.00	0.3326			
									period	2	1.15	0.5624	0.8860	0.5143	0.9714
	Swim speed	8	0.639	0.068	0.659	0.079	0.586	0.060	ID	7	7.00	0.4294			
									period	2	1.12	0.5711	0.7051	0.5102	0.6287

Generalized estimating equations (GEE) fitted to behavioral data (Figure 2), using *ID* and *Period* as predictor variables. Data were modeled as repeated measurements with *ID* as the within-subject factor and *Period* as the between-subject factor. P1, P2, and P3: First, second, and third 2.5 min period, respectively. Significant values ($p < 0.05$) are shown in bold.

habituation.[7,8] With the current work, we present evidence of operant conditioning in cnidarians, a type of associative learning that has previously only been clearly demonstrated in bilaterian animals, e.g., vertebrates, arthropods, and mollusks.[2,10]

Operant conditioning, originally coined by B.S. Skinner (1938),[33] is defined as learning the effects of one's own actions to avoid something aversive or obtain something of value.[2,30] An immense variety of complexity in operant learning can be observed throughout the metazoans, from rats controlling levers to modulation of the biting reflex in *Aplysia*.[30] Obviously, an animal with a relatively simple nervous system and limited motor effectors, such as *Aplysia* or *T. cystophora*, will never be able to perform on the level of highly cognitive and agile animals, such as rats or mice. This accentuates the importance of utilizing sensory input (CS and US) that can be correctly interpreted and responded to by the experimental organism. It follows that the tested behavioral output must be evaluated based on the motor capabilities of the animal and its natural behavioral repertoire.[34,35] In the present work, *T. cystophora* learned to associate low-contrast objects with increased risk of collision. Great care was taken to ensure that the experimental sensory input and the evaluation of behavioral output conformed to the capabilities of the experimental animal. Using this adaptive approach, we show that the basis of learning to respond adequately to contrast:distance in *T. cystophora* is concurrent visual and mechanosensory stimuli.

In the present study, we define the post-training responses of *T. cystophora* as operant conditioning due to the generally increased sensitivity to lower-contrast objects. In practice, however, it is often difficult to separate operant and classical conditioning. According to the "two-factor theory," both classical and operant conditioning are necessary for avoidance responses to occur.[36,37] Through classical training in the *ex vivo* experiments, *T. cystophora* learned to associate the aversive stimulus of "colliding" (US) with the presented "obstacle" (CS). Following the training, the animal showed escape response to the CS, to "reduce the fear" of the US (operant conditioning).[36,37] It is obvious that the broad field of animal learning has brought about a great number of theoretical paradigms seeking to explain the mechanisms of learning. In addition to the two-factor theory, which we find appropriate for the current study, other theories have been proposed to explain the functional basis of avoidance learning, such as "cognitive theory,"[36,38] and "world-learning."[39]

Avoidance of genuinely threatening stimuli (like the prop roots) is a key characteristic of adaptive fear,[40] and the innate OAB in

Please cite this article in press as: Bielecki et al., Associative learning in the box jellyfish *Tripedalia cystophora*, Current Biology (2023), https://doi.org/10.1016/j.cub.2023.08.056

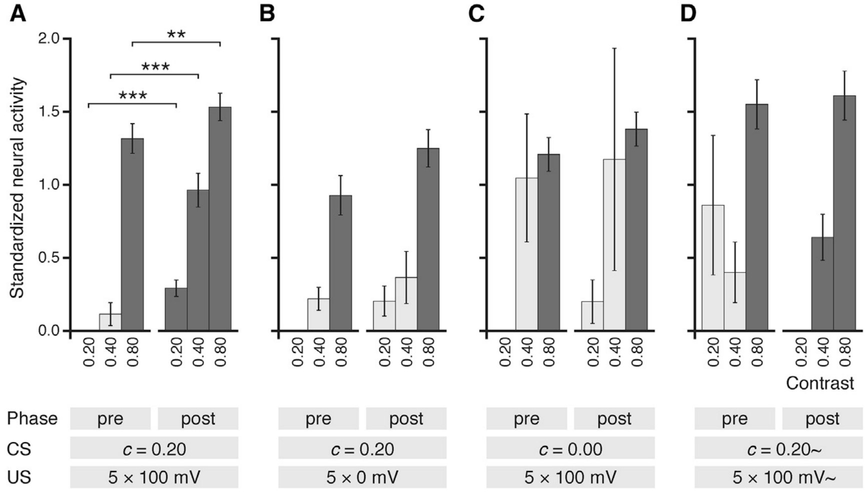

Figure 3. Classical conditioning in isolated rhopalia using weak electrical stimulation

(A) A key component in the obstacle avoidance response is an increase in the swim pacemaker frequency. In the neurophysiological assays, this frequency was monitored in response to moving obstacles with three levels of contrast ($c = 0.20$, $c = 0.40$, and $c = 0.80$). In the pre-training phase (pre), the pacemaker cells only responded to the high-contrast stimulus. After classical training (post) using the low-contrast obstacle ($c = 0.20$) as conditioned stimulus (CS), and a mechanosensory signal mimic (100 mV 50 ms single square pulse) as unconditioned stimulus (US), the rhopalia responded to low-, mid-, and high-contrast obstacles. Also, the response to the high-contrast obstacle was significantly higher in the post-training phase. These results confirm that operant learning occurs within the rhopalial nervous system (RNS) by a combination of visual and mechanical stimuli.

(B) When using the visual CS alone, without mechanosensory US, no response to contrasts lower than $c = 0.80$ was induced in the post-training phase. These results confirm that learning is absent with visual stimulation alone.

(C) Training using the mechanosensory US only did not increase responsiveness in the post-training phase either (responses to the high-contrast obstacles only). These results confirm that learning is absent with mechanical stimulation alone.

(D) Training using temporally uncoupled (unpaired) CS and US did not increase responsiveness in the post-training phase. Bars denote modeled standardized neural activity (y_m) ± SE of the modeled peak (Tables 3 and 4). Gray and light gray bars symbolize significant and not significant results, respectively, as defined in the STAR Methods. Asterisks denote levels of significance of differences when pre- and post-training experiments were compared for a given combination of CS and US (**$p < 0.01$, and ***$p < 0.0001$). Unpaired CS and US marked by tilde (~). See also Figures S1–S5.

box jellyfish is a species-specific defense reaction (SSDR), which is more easily learned.[34] The two-factor operant conditioning in *T. cystophora* occurs within 7.5 min, including an average of 7.55 contacts with the behavioral arena wall (Figure 2A). In the *ex vivo* classical training, 5 min and 5 "contacts" (weak electric pulses) sufficed to induce significantly increased responsiveness to low-contrast obstacles (Figures 3 and S1). Even though it may not be possible to make direct comparisons due to differences in the experimental protocols, especially with regards to the nature/strength of the stimuli, the time and number of trials required for learning in *T. cystophora* are similar to requirements in insects,[41] possibly indicating evolutionarily conserved underlying neuronal mechanisms. Our results emphasize the importance of targeted SSDRs especially when working with animals with relatively simple nervous systems since such systems are likely to have a higher proportion of innate behaviors and less plasticity.[42] The full potential of their natural learning capacity can only be revealed by addressing active behaviors (such as typical SSDRs) using natural stimuli. If animals are trained using unnatural CS and US (SSDR non-conform), the results might be behavioral changes indicative of learning, but this informs little about the functional implication for the system in question and might induce several artifacts and unnatural behavior. In fact, this has been the key problem with previous work testing associative learning in cnidarians. Haralson et al. (1975) tested associative learning in a sea anemone using exceedingly strong US stimuli (electric shocks of 32 V repeated 50 times of 5 s duration) and a CS (bright flashes of light), which will not occur in their natural habitat and have no known behavioral relevance for the tested species of sea anemone.[11] In a recent similar study, Botton-Amiot and colleagues delivered electric shocks of 6 V repeated 120 times of 1 s duration to the sea anemone *Nematostella vectensis* using short periods of light as CS.[12] In both studies, behavioral changes were seen that are in line with associative learning, but the highly unnatural stimuli make it questionable if it takes place in a naturally behaving animal and thus if it has behavioral relevance.[11,12]

The present study fulfills all requirements of manipulated SSDRs. Both the behavioral CS (bars on the perimeter wall of the behavioral arena) and the US (collisions with the wall) are naturally occurring events, which we realistically mimicked in the *ex vivo* experiments.

The *ex vivo* approach is comparable to work involving *Aplysia*, where electrical stimulation directly to the esophageal nerve En^2 mimicked a food reward and induced increased post-training bite rate.[30] This and other invertebrate studies have suggested that operant conditioning modulates central convergent behavior-initiating or switching neurons by altering their biophysical membrane properties.[43] The cellular mechanisms involved in box jellyfish operant learning are beyond the scope of the present work, but our results are congruent with learning-induced plasticity of a central pivotal cell cluster, since mechanosensory signals (or electrical mechanosensory signal mimics) reach the rhopalial pacemaker cells through the bidirectional epidermal stalk nerve and alter the OAB. Biophysical changes to the membrane properties of a central convergent cell cluster are further supported by the observation that *T. cystophora* did not exclusively respond to the training CS ($c = 0.20$) in the post-training phase. Instead, we found a progressive increase in responsiveness to lower-contrast obstacles (Figures 3A and S1; Table 3 and 4). The training US parameter (50 ms of 100 mV at 100 nA) potentially induces cellular plasticity to a specific level, which is subsequently reflected in the post-training responsiveness. It is thereby possible that the pacemaker cell cluster constitutes a convergence point similar to the buccal neuron B51 neuron reported in *Aplysia*.[30,43] This notion is also supported by the

Please cite this article in press as: Bielecki et al., Associative learning in the box jellyfish *Tripedalia cystophora*, Current Biology (2023), https://doi.org/10.1016/j.cub.2023.08.056

Table 3. Pacemaker response to pre- and post-training treatment sequences

Training treatment	Phase	Contrast (c)	F (model)	p (model)	Reaction (y_m)	SE (y_m)	p($y_m = 0$)	a	SE (a)	p($a = 0$)	b	SE (b)	p($b = 0$)	t_{peak} [s]
CS $c = 0.20$ US 5 × 100mV	pre-training	0.20	–	–	–	–	–	–	–	–	–	–	–	–
		0.40	0.90	0.4390	0.11	0.08	0.1572	76.2	125.9	0.5450	52.49	86.31	0.5431	17.36
		0.80	**73.87**	**<0.0001**	**1.32**	**0.10**	**<0.0001**	**444.5**	**94.9**	**<0.0001**	**535.7**	**114.4**	**<0.0001**	**6.28**
	post-training	0.20	**8.76**	**<0.0001**	**0.29**	**0.06**	**<0.0001**	8.27	4.54	0.0688	9.77	5.35	0.0678	**6.68**
		0.40	**31.37**	**<0.0001**	**0.96**	**0.12**	**<0.0001**	323.9	108.8	0.0029	388.9	130.2	0.0028	**6.35**
		0.80	**113.14**	**<0.0001**	**1.53**	**0.10**	**<0.0001**	**252.1**	**44.99**	**<0.0001**	**308.5**	**55.03**	**<0.0001**	**5.98**
CS $c = 0.20$ US 5 × 0mV	pre-training	0.20	–	–	–	–	–	–	–	–	–	–	–	–
		0.40	3.04	0.0283	0.22	0.08	0.0069	39.84	37.2	0.2842	40.85	38.16	0.2844	9.50
		0.80	**21.65**	**<0.0001**	**0.93**	**0.14**	**<0.0001**	759.3	295.7	0.0102	917.9	357.4	0.0102	**6.22**
	post-training	0.20	1.60	0.1873	0.20	0.11	0.0544	58.01	72.65	0.4246	40.84	51.46	0.4274	16.95
		0.40	1.94	0.1214	0.36	0.18	0.0442	545.6	647.9	0.3997	238.8	283.20	0.3991	25.65
		0.80	**41.87**	**<0.0001**	**1.25**	**0.13**	**<0.0001**	**638.1**	**180.9**	**0.0004**	**769.6**	**218.50**	**0.0004**	**6.26**
CS $c = 0.00$ US 5 × 100mV	pre-training	0.20	–	–	–	–	–	–	–	–	–	–	–	–
		0.40	2.74	0.0424	1.05	0.44	0.0174	3.8×10^4	3.1×10^4	0.2165	4.3×10^4	3.5×10^4	0.2164	7.62
		0.80	**47.81**	**<0.0001**	**1.21**	**0.12**	**<0.0001**	**496.20**	**130.8**	**0.0001**	**586.10**	**154.50**	**0.0001**	**6.68**
	post-training	0.20	0.81	0.4884	0.20	0.15	0.1867	370.90	677.2	0.5839	307.30	561.50	0.5842	13.75
		0.40	1.80	0.1451	1.17	0.76	0.1241	2.1×10^4	2.6×10^4	0.4036	2.2×10^4	2.6×10^4	0.4042	9.75
		0.80	**60.73**	**<0.0001**	**1.38**	**0.12**	**<0.0001**	**395.20**	**99.96**	**<0.0001**	**471.00**	**119.30**	**<0.0001**	**6.50**
CS $c = 0.20$ US 5 × 100mV unpaired	pre-training	0.20	1.60	0.1896	0.86	0.48	0.0750	4956.0	7176.8	0.4902	5991.1	8665.5	0.4897	6.22
		0.40	1.70	0.1617	0.40	0.21	0.0517	274.0	365.0	0.4535	327.0	435.0	0.4535	6.48
		0.80	**35.06**	**<0.0001**	**1.55**	**0.17**	**<0.0001**	272.9	97.81	0.0055	326.0	117.10	0.0057	**6.45**
	post-training	0.20	–	–	–	–	–	–	–	–	–	–	–	–
		0.40	**5.13**	**0.0019**	**0.64**	**0.16**	**0.0001**	6.35	5.02	0.2074	8.09	6.15	0.1898	**5.17**
		0.80	**37.32**	**<0.0001**	**1.61**	**0.17**	**<0.0001**	124.0	45.7	0.0071	151.5	55.89	0.0072	**6.01**

Results of neurophysiological assays with lower lens eyes (LLE) of *T. cystophora* medusae exposed to visual stimuli, representing three levels of contrast (c). Equation 5 (STAR Methods) was fitted to the standardized neural activity (Figures S1–S4), and the model's parameters (y_m, a, and b) were used to describe the time trends in spike frequencies. F(model) tests the overall fit of the model to data (indicated by the p value for the model). y_m denotes the maximum pacemaker reaction to the stimulus, while a and b define the location and width of the peak. t_{peak} denotes the time from the onset of visual stimulation and until the neural activity reaches its maximum. Bold values of t_{peak} mark that the underlying model used to estimate t_{peak} was significant. p values indicate the significance of the individual test statistics. Parameter values, which were significant after a sequential Bonferroni adjustment,[32] are shown in bold. Missing values (indicated by –) were due to lack of convergence of the algorithm (i.e., no response to the stimulus). See also Figures S1–S5.

Table 4. Analysis of responses to pre- vs. post-training treatment sequences

		Model fit		Difference between pre- and post-training reactions		
Training treatment	Contrast	F	p	Reaction (y'_m)	SE (y'_m)	p($y'_m = 0$)
CS $c = 0.20$ US 5 × 100mV	0.20	**7.03**	**<0.0001**	**0.2915**	**0.0564**	**<0.0001**
	0.40	**21.88**	**<0.0001**	**0.7767**	**0.1491**	**<0.0001**
	0.80	**112.38**	**<0.0001**	**0.3592**	**0.1186**	**0.0025**
CS $c = 0.20$ US 5 × 0mV	0.20	1.44	0.2170	0.4022	0.2045	0.0492
	0.40	1.73	0.1252	-0.1686	0.1187	0.1555
	0.80	**38.93**	**<0.0001**	0.3582	0.1605	0.0257
CS $c = 0.00$ US 5 × 100mV	0.20	0.60	0.6615	0.1998	0.1521	0.1890
	0.40	1.68	0.1362	0.3031	0.1993	0.1283
	0.80	**65.44**	**<0.0001**	0.2279	0.1431	0.1113
CS $c = 0.20$ US 5 × 100mV Unpaired	0.20	1.68	0.1376	0.8119	0.6144	0.1869
	0.40	2.68	0.0148	0.3327	0.3072	0.2793
	0.80	**42.38**	**<0.0001**	0.1998	0.2144	0.3518

Effect of training on the pacemaker reaction to visual stimuli with contrast $c = 0.20$, 0.40, or 0.80, measured as the difference between pre-training and post-training values of y_m (denoted y_m'). A positive value of y_m' indicates that responsiveness increased after training. P denotes the significance of the overall fit of the model and the estimated values of y_m'. Values shown in bold are significant after a sequential Bonferroni adjustment.[32] See also Figures S1–S5.

recently proposed idea of oscillators' and servomechanisms' involvement in cognition.[44] Interconnected oscillatory clusters can explain at least some of the visual information processing functions of the *T. cystophora* RNS. Consequently, it would be tempting to suggest changes in oscillatory frequencies in central convergence clusters in response to avoidance learning. However, further investigations into this topic are warranted before any conclusions can be drawn.

As described above, the behavioral assays and the neurophysiological experiments confirm operant conditioning in the box jellyfish *T. cystophora*, which, in contrast to habituation and sensitization, is considered associative learning.[1,2] Such operant conditioning has previously been considered to require advanced nervous systems including a conventional centralized brain.[42] This notion is now challenged, since the box jellyfish has a dispersed nervous system and lacks a centralized brain. The basal phylogenetic position of cnidarians as a sister group to bilaterians, combined with our results, point at the intriguing suggestion that even highly advanced neuronal processes, like operant conditioning, reside within all nervous systems and are potentially a fundamental property of neuronal circuitry. Furthermore, since we demonstrate the full learning capacity of isolated rhopalia, we placed the plasticity of the neuronal processing within the RNS. The simplicity of the RNS,[18] combined with inducible circuit plasticity, makes it an attractive model for studying systems-level learning and memory formation.

STAR★METHODS

Detailed methods are provided in the online version of this paper and include the following:

- KEY RESOURCES TABLE
- RESOURCE AVAILABILITY
  - Lead contact
  - Materials availability
  - Data and code availability
- EXPERIMENTAL MODEL AND SUBJECT DETAILS
- METHOD DETAILS
  - Behavioral experiments
  - Behavioral protocol
  - Neurophysiological experiments – classical training
  - *Ex vivo* sample preparation
  - Extracellular recording
  - Visual stimulus
  - Treatment protocol
- QUANTIFICATION AND STATISTICAL ANALYSIS
  - Analysis of behavioral data
  - Analysis of neurophysiological data

SUPPLEMENTAL INFORMATION

Supplemental information can be found online at https://doi.org/10.1016/j.cub.2023.08.056.

ACKNOWLEDGMENTS

The authors are grateful for the technical assistance offered by Mathias Hoppe, Ingo Klein, Olaf Wendt, and Holger Voigt (Kiel University) and the help from the members of the Sensory Biology Group (University of Copenhagen) with maintaining the cultures. We acknowledge the three anonymous reviewers who helped tighten the manuscript. Funded by the Deutsche Forschungsgemeinschaft (DFG, German Research Foundation) – Project-ID 434434223 – SFB 1461 (J.B.), Danish Research Council (DFF) – grant no. 4181-00398 (A.G.), and The Villum Foundation – grant no. 40837 (A.G.).

AUTHOR CONTRIBUTIONS

J.B. and A.G. developed the concept for the paper. A.G. and S.K.D.N. conceptualized, planned, performed, and analyzed the data of the behavioral experiments. J.B. conceptualized, planned, performed, and analyzed the data of the neurophysiological experiments. G.N. performed statistical data analysis of all experiments and developed the algorithm used for analyzing the neurophysiological experiments. J.B. and A.G. wrote the manuscript and designed the figures. All authors contributed to finalizing the manuscript.

DECLARATION OF INTERESTS

The authors declare no competing interests.

Received: January 5, 2023
Revised: July 17, 2023
Accepted: August 18, 2023
Published: September 22, 2023

REFERENCES

1. Skinner, B.F. (1981). Selection by Consequences. Science *213*, 501–504. https://doi.org/10.1126/science.7244649.
2. Perry, C.J., Barron, A.B., and Cheng, K. (2013). Invertebrate learning and cognition: relating phenomena to neural substrate: Invertebrate learning and cognition. WIREs Cogn Sci *4*, 561–582. https://doi.org/10.1002/wcs.1248.
3. Raji, J.I., and Potter, C.J. (2021). The number of neurons in Drosophila and mosquito brains. PLoS One *16*, e0250381, https://doi.org/10.1371/journal.pone.0250381.
4. Goshen, I. (2014). The optogenetic revolution in memory research. Trends Neurosci. *37*, 511–522. https://doi.org/10.1016/j.tins.2014.06.002.
5. Kandel, E.R. (2001). The Molecular Biology of Memory Storage: A Dialogue Between Genes and Synapses. Science *294*, 1030–1038. https://doi.org/10.1126/science.1067020.
6. Sasakura, H., and Mori, I. (2013). Behavioral plasticity, learning, and memory in C. elegans. Curr. Opin. Neurobiol. *23*, 92–99. https://doi.org/10.1016/j.conb.2012.09.005.
7. Brace, R.C., and Santer, S.-J. (1991). Experimental habituation of aggression in the sea anemone Actinia equina. In Coelenterate Biology: Recent Research on Cnidaria and Ctenophora, R.B. Williams, P.F.S. Cornelius, R.G. Hughes, and E.A. Robson, eds. (Springer Netherlands), pp. 533–537. https://doi.org/10.1007/978-94-011-3240-4_75.
8. Rushforth, N.B., Krohn, I.T., and Brown, L.K. (1964). Behavior in *Hydra* : Inhibition of the Contraction Responses of *Hydra pirardi*. Science *145*, 602–604. https://doi.org/10.1126/science.145.3632.602.
9. Hodgson, V.S. (1981). Conditioning as a factor in the symbiotic feeding relationship of sea anemones and anemone fishes. In Proceedings of the International Coral Reef Symposium, pp. 553–561.
10. Cheng, K. (2021). Learning in Cnidaria: A systematic review. Learn. Behav. *49*, 175–189. https://doi.org/10.3758/s13420-020-00452-3.
11. Haralson, J.V., Groff, C.I., and Haralson, S.J. (1975). Classical conditioning in the sea anemone, Cribrina xanthogrammica. Physiol. Behav. *15*, 455–460. https://doi.org/10.1016/0031-9384(75)90259-0.
12. Botton-Amiot, G., Martinez, P., and Sprecher, S.G. (2023). Associative learning in the cnidarian *Nematostella vectensis*. Proc. Natl. Acad. Sci. USA *120*, e2220685120, https://doi.org/10.1073/pnas.2220685120.
13. Garm, A., O'Connor, M., Parkefelt, L., and Nilsson, D.-E. (2007). Visually guided obstacle avoidance in the box jellyfish Tripedalia cystophora and Chiropsella bronzie. J. Exp. Biol. *210*, 3616–3623. https://doi.org/10.1242/jeb.004044.
14. Lewis, C., and Long, T.A.F. (2005). Courtship and reproduction in Carybdea sivickisi (Cnidaria: Cubozoa). Mar. Biol. *147*, 477–483. https://doi.org/10.1007/s00227-005-1602-0.
15. Garm, A., Oskarsson, M., and Nilsson, D.-E. (2011). Box Jellyfish Use Terrestrial Visual Cues for Navigation. Curr. Biol. *21*, 798–803. https://doi.org/10.1016/j.cub.2011.03.054.
16. Nilsson, D.-E., Gislén, L., Coates, M.M., Skogh, C., and Garm, A. (2005). Advanced optics in a jellyfish eye. Nature *435*, 201–205. https://doi.org/10.1038/nature03484.
17. Pearse, J.S., and Pearse, V.B. (1978). Vision of Cubomedusan Jellyfishes. Science *199*, 458. https://doi.org/10.1126/science.22934.
18. Skogh, C., Garm, A., Nilsson, D.-E., and Ekström, P. (2006). Bilaterally symmetrical rhopalial nervous system of the box jellyfish Tripedalia cystophora. J. Morphol. *267*, 1391–1405. https://doi.org/10.1002/jmor.10472.
19. Nielsen, S.K.D., Koch, T.L., Wiisbye, S.H., Grimmelikhuijzen, C.J.P., and Garm, A. (2021). Neuropeptide expression in the box jellyfish *Tripedalia cystophora* —New insights into the complexity of a "simple" nervous system. J. Comp. Neurol. *529*, 2865–2882.
20. Parkefelt, L., Skogh, C., Nilsson, D.-E., and Ekström, P. (2005). Bilateral symmetric organization of neural elements in the visual system of a coelenterate, *Tripedalia cystophora* (Cubozoa). J. Comp. Neurol. *492*, 251–262. https://doi.org/10.1002/cne.20658.
21. Satterlie, R.A., and Spencer, A.N. (1979). Swimming control in a cubomedusan jellyfish. Nature *281*, 141–142. https://doi.org/10.1038/281141a0.
22. Garm, A., and Mori, S. (2009). Multiple photoreceptor systems control the swim pacemaker activity in box jellyfish. J. Exp. Biol. *212*, 3951–3960. https://doi.org/10.1242/jeb.031559.
23. Buskey, E. (2003). Behavioral adaptations of the cubozoan medusa Tripedalia cystophora for feeding on copepod (Dioithona oculata) swarms. Mar. Biol. *142*, 225–232. https://doi.org/10.1007/s00227-002-0938-y.
24. Stewart, S.E. (1996). Field behavior of *tripedalia cystophora* (class cubozoa). Mar. Freshw. Behav. Physiol. *27*, 175–188. https://doi.org/10.1080/10236249609378963.
25. Garm, A., Hedal, I., Islin, M., and Gurska, D. (2013). Pattern- and contrast-dependent visual response in the box jellyfish Tripedalia cystophora. J. Exp. Biol. *216*, 4520–4529. https://doi.org/10.1242/jeb.091934.
26. Kirk, J.T.O. (1985). Effects of suspensoids (turbidity) on penetration of solar radiation in aquatic ecosystems. Hydrobiologia *125*, 195–208. https://doi.org/10.1007/BF00045935.
27. Garm, A., Bielecki, J., Petie, R., and Nilsson, D.-E. (2012). Opposite Patterns of Diurnal Activity in the Box Jellyfish *Tripedalia cystophora* and *Copula sivickisi*. Biol. Bull. *222*, 35–45. https://doi.org/10.1086/BBLv222n1p35.
28. Garm, A., and Bielecki, J. (2008). Swim pacemakers in box jellyfish are modulated by the visual input. J. Comp. Physiol. *194*, 641–651. https://doi.org/10.1007/s00359-008-0336-0.
29. Satterlie, R.A., and Nolen, T.G. (2001). Why do cubomedusae have only four swim pacemakers? J. Exp. Biol. *204*, 1413–1419. https://doi.org/10.1242/jeb.204.8.1413.
30. Brembs, B., Lorenzetti, F.D., Reyes, F.D., Baxter, D.A., and Byrne, J.H. (2002). Operant Reward Learning in *Aplysia* : Neuronal Correlates and Mechanisms. Science *296*, 1706–1709. https://doi.org/10.1126/science.1069434.
31. Reynolds, J.N., Hyland, B.I., and Wickens, J.R. (2001). A cellular mechanism of reward-related learning. Nature *413*, 67–70. https://doi.org/10.1038/35092560.
32. Holm, S. (1979). A Simple Sequentially Rejective Multiple Test Procedure. Scand. J. Stat. *6*, 65–70.
33. Skinner, B.F. (1938). The behavior of organisms: an experimental analysis (Prentice-Hall).
34. Bolles, R.C. (1970). Species-specific defense reactions and avoidance learning. Psychol. Rev. *77*, 32–48. https://doi.org/10.1037/h0028589.
35. Freas, C.A., and Cheng, K. (2022). Neuroecology beyond the brain: learning in Echinodermata. Learn. Behav. *50*, 20–36. https://doi.org/10.3758/s13420-021-00492-3.
36. Mazur, J.E. (2016). Learning and Behavior. (Routledge).
37. Mowrer, O.H. (1947). On the dual nature of learning—a re-interpretation of "conditioning" and "problem-solving. Harv. Educ. Rev. *17*, 102–148.
38. Seligman, M.E., and Johnston, J.C. (1973). A cognitive theory of avoidance learning. In Contemporary approaches to conditioning and learning (V. H. Winston & Sons), p. 321. xii, 321–xii.
39. Colomb, J., and Brembs, B. (2010). The biology of psychology: Simple conditioning? Commun. Integr. Biol. *3*, 142–145. https://doi.org/10.4161/cib.3.2.10334.

Please cite this article in press as: Bielecki et al., Associative learning in the box jellyfish *Tripedalia cystophora*, Current Biology (2023), https://doi.org/10.1016/j.cub.2023.08.056

40. Krypotos, A.-M., Effting, M., Kindt, M., and Beckers, T. (2015). Avoidance learning: a review of theoretical models and recent developments. Front. Behav. Neurosci. *9*, 189. https://doi.org/10.3389/fnbeh.2015.00189.
41. Brembs, B., and Heisenberg, M. (2000). The Operant and the Classical in Conditioned Orientation of *Drosophila melanogaster* at the Flight Simulator. Learn. Mem. *7*, 104–115. https://doi.org/10.1101/lm.7.2.104.
42. Ginsburg, S., and Jablonka, E. (2010). The evolution of associative learning: A factor in the Cambrian explosion. J. Theor. Biol. *266*, 11–20. https://doi.org/10.1016/j.jtbi.2010.06.017.
43. Brembs, B. (2003). Operant conditioning in invertebrates. Curr. Opin. Neurobiol. *13*, 710–717. https://doi.org/10.1016/j.conb.2003.10.002.
44. Cheng, K. (2022). Oscillators and servomechanisms in orientation and navigation, and sometimes in cognition. Proc. Biol. Sci. *289*, 20220237, https://doi.org/10.1098/rspb.2022.0237.
45. Garm, A., Coates, M.M., Gad, R., Seymour, J., and Nilsson, D.-E. (2007). The lens eyes of the box jellyfish Tripedalia cystophora and Chiropsalmus sp. are slow and color-blind. J. Comp. Physiol. *193*, 547–557. https://doi.org/10.1007/s00359-007-0211-4.
46. Coates, M.M., Garm, A., Theobald, J.C., Thompson, S.H., and Nilsson, D.-E. (2006). The spectral sensitivity of the lens eyes of a box jellyfish, Tripedalia cystophora (Conant). J. Exp. Biol. *209*, 3758–3765. https://doi.org/10.1242/jeb.02431.
47. Bielecki, J., Zaharoff, A.K., Leung, N.Y., Garm, A., and Oakley, T.H. (2014). Ocular and Extraocular Expression of Opsins in the Rhopalium of Tripedalia cystophora (Cnidaria: Cubozoa). PLoS One *9*, e98870–e98879. https://doi.org/10.1371/journal.pone.0098870.
48. Bielecki, J., Nachman, G., and Garm, A. (2013). Swim pacemaker response to bath applied neurotransmitters in the cubozoan Tripedalia cystophora. J. Comp. Physiol. *199*, 785–797. https://doi.org/10.1007/s00359-013-0839-1.
49. Govardovskii, V.I., Fyhrquist, N., Reuter, T., Kuzmin, D.G., and Donner, K. (2000). In search of the visual pigment template. Vis. Neurosci. *17*, 509–528. https://doi.org/10.1017/S0952523800174036.
50. Nachman, G., and Gotoh, T. (2015). Modeling the Effects of Constant and Variable Temperatures on the Vital Rates of an Age-Stage-and Sex-Structured Population by Means of the SANDY Approach. Environ. Entomol. *44*, 821–834. https://doi.org/10.1093/ee/nvv056.

Please cite this article in press as: Bielecki et al., Associative learning in the box jellyfish *Tripedalia cystophora*, Current Biology (2023), https://doi.org/10.1016/j.cub.2023.08.056

STAR★METHODS

KEY RESOURCES TABLE

REAGENT or RESOURCE	SOURCE	IDENTIFIER
Deposited data		
Neurophysiological data	Mendelay Data	https://doi.org/10.17632/csgymw8kjk.1
Experimental models: Organisms/strains		
Tripedalia cystophora (wt)	Cultures (CPH, Kiel Lab)	N/A
Software and algorithms		
MATLAB	MathWorks, Natick, MA, USA	N/A
LabView, custom VI	National Instruments	N/A
IGOR Pro 6.37 Neuromatic plug-in	WaveMetrics Inc, Lake Oswego, OR, USA	N/A
PROC GLM in SAS OnDemand for Academics	SAS Institute 2020	N/A
Other		
photometer X1-5 optometer with a RW-3703-5 detector head	Gigahertz-Optics, Germany	N/A
spectrophotometer ILT900W	International Light Technologies, Peabody, MA, USA	N/A
Sony Handycam DCR-HC40	Sony, Tokyo, Japan	N/A
10-2F EXT amplifier	NPI electronic, Tamm, Germany	N/A
A/D converter NI6343	National Instruments	N/A
LED projector ML750 DLP	Optoma, Fremont, CA, USA	N/A
USB-650 spectrometer fitted with a P400-2-VIS/NIR fiber	OceanOptics, Ostfildern, Germany	N/A

RESOURCE AVAILABILITY

Lead contact

Requests for further information or resources should be directed to the lead contact, Jan Bielecki, jan@bielecki.dk.

Materials availability

This study did not generate any new unique reagents.

Data and code availability

- The data reported in this paper is publicly available at Mendeley Data repository: https://doi.org/10.17632/csgymw8kjk.1.
- Any additional information required to reanalyze the data reported in this paper is available from the lead contact upon request.

EXPERIMENTAL MODEL AND SUBJECT DETAILS

All animals used for the behavioral experiments were adult medusae (7-9 mm in bell diameter) obtained from cultures at University of Copenhagen, Denmark, originating from the mangroves near La Parguera, Puerto Rico. The animals were cultured in 250 L tanks with recycled seawater at 27°C-28°C and 35-37 PSU. The light:dark cycle in the culture tanks was 9:15 h. The medusae were fed SELCO enriched *Artemia* nauplii daily and reached adult size in approximately 2 months. A total of 27 medusae were used in the behavioral trials. All animals used for the neurophysiological experiments were adult medusae harvested from a culture, which also originated

Please cite this article in press as: Bielecki et al., Associative learning in the box jellyfish *Tripedalia cystophora*, Current Biology (2023), https://doi.org/10.1016/j.cub.2023.08.056

from Puerto Rico, but maintained at Kiel University, Germany. They were cultured under similar conditions as in Copenhagen. A total of 40 medusae were used for the neurophysiological trials.

METHOD DETAILS

Behavioral experiments

Behavioral arena

The behavioral arena was designed as described in previous work.[25] It was an opaque round tank with a diameter of 16 cm and filled with water from the culture tank to minimize stress, which can be induced by moving animals to water with even small changes in salinity and/or chemical composition. The water depth was ~15 cm and the water was kept at 28°C by placing the tank on a heating plate. Light came directly from above using a 10 W white LED lamp (LUXO, Ovello LED work lamp) situated approximately 50 cm above the center of the tank, thereby creating an even illumination of the behavioral arena. The intensity at the surface was 8.5 Wm^{-2} measured with a handheld photometer (X1-5 optometer with a RW-3703-5 detector head, Gigahertz-Optics, Germany). The inside of the tank wall accommodated a changeable cylinder of hard plastic with the different visual scenes used. The visual scenes were either alternating 2 cm wide vertical black and white stripes, alternating gray and white stripes (the black and gray stripes mimicking prop roots) or a uniformly gray wall. The contrast between the black and white stripes was 0.93, and it was 0.39 for the gray and white stripes. The contrast (c) was calculated as $c = \frac{I_w - I_g}{I_w + I_g}$, where I_g is the intensity reflected from the gray or black stripes and I_w is the intensity reflected from the white stripes, both corrected by the absorption spectrum of the 500 nm opsin present in the lower lens eyes.[45–47] The gray tone used for the visually uniform wall matched the average intensity of the white and black striped wall. The intensities were all measured from 350 to 700 nm using a spectrophotometer (ILT900W, International Light Technologies, Peabody, MA, USA) with the sensor held perpendicular to the wall at a distance of 1 cm and 1 cm below the surface.

Behavioral protocol

At the onset of each 30 min behavioral trial a naïve medusa was transferred from the culture tank to the center of the arena using a Petri dish. It was left to adjust for approx. 2 min, after which it had re-extended its tentacles and swam with a normal pulse rate (0.5–1.5 Hz). Then a cover was placed above the arena, keeping the medusa in darkness for 22.5 min, allowing the medusa to rest on the bottom of the arena.[27] When the cover was removed, the medusa started swimming within 1-2 min and its behavior was recorded from above for 7.5 min using a video camera (Sony Handycam DCR-HC40, Sony, Tokyo, Japan). Twelve medusae were tested with the gray and white stripes, seven medusae with black and white stripes, and eight medusae with uniform gray wall in the arena.

Neurophysiological experiments – classical training

Since an OAB is characterized by a rapid increase in swim contractions, resulting in burst swimming, the signal frequencies of the swim pacemaker can be used for analyzing avoidance behavior. Swim pacemaker signals are generated in the RNS and can be recorded from the efferent epidermal stalk nerve of an isolated rhopalium.[21,28] This offers the advantage of experimenting on an isolated rhopalium positioned to face a projecting screen, thereby providing complete control of the images presented to the LLE (Figures 1D and S5A). Since successful learning of the contrast:distance in *T. cystophora* may not only require visual stimuli, but also a concurrent mechanical stimulus, using isolated rhopalia poses an experimental challenge. We reason that an electrical stimulation will reach the pacemaker cell clusters as a mechanosensory mimic when applied to the suction electrode that records the swim pacemaker signals from the bidirectional epidermal stalk nerve.[29] The swim pacemaker signal originates from the pacemaker cell cluster as a convergent signal, and is an integrated signal of about 45-50 ms duration.[29] Applying sensory stimulation by means of direct electrical stimulation of the CNS is similar to operant conditioning in *Aplysia*[30] and rodents.[31]

Ex vivo sample preparation

Initially, an adult medusa was pipetted from the culturing tank and placed in a seawater-filled Petri dish, whereupon the water was removed until the animal remained immobile when manipulated. The rhopalial stalk was then transected approximately midway between the attachment points of the bell and the rhopalium using a pair of fine scissors. The isolated rhopalium was transferred to a custom-made recording chamber (w:d:h = 30:18:12 mm containing 0.22 μm filtered seawater from the culturing tank. The recording chamber was kept at a close-to-constant temperature of 28 ± 0.5°C.

Extracellular recording

A custom-made glass capillary suction electrode with a pore size of 5-10 μm (150-200 kΩ) was attached to the transected epidermal stalk nerve and the pacemaker signals were recorded relative to a reference electrode (single ended recordings). The signals were amplified (×1000, 10-2F EXT amplifier, NPI electronic, Tamm, Germany) and filtered through high- and low-pass filters (30 and 500 Hz), and a notch filter (50 Hz). The signals were recorded on a PC using an A/D converter (National Instruments NI6343) controlled by a customized Virtual Instrument (LabView, National Instruments). The recordings were analyzed using Igor Pro software version 6.37 with the Neuromatic plugin (WaveMetrics Inc, Lake Oswego, OR, USA), where true swim pacemaker signals were filtered from more action-like potentials.[48] The timestamp of the individual swim pacemaker signals was extracted and the effect of the visual stimulus was evaluated as described below.

Visual stimulus

The LLE in each preparation ($N = 10$) was presented with a moving gray bar as a visual mimic of the obstacles (prop roots) in the natural habitat of the jellyfish. This was done by projecting an image onto a screen on one side of the recording chamber. A series of lenses focused the image from an LED projector (ML750 DLP, Optoma, Fremont, CA, USA) onto the screen. The rhopalium was held by a suction micropipette and placed on a cover glass ledge in front of the middle of the screen at a distance of 2 mm. The screen had an inclination of 60° relative to vertical matching the angle of the LLE on a freely suspended rhopalium,[15] which ensured that the screen was perpendicular to the optical axis of the LLE. A photodiode monitored the computer screen to record the movement of the obstacle, which enabled timing of the visual stimulus to the swim pacemaker recordings. The projected image was 16 mm wide (w:h = 16:12 mm) and at a distance of 2 mm from the LLE, covering approximately 150° horizontally and 120° vertically of the 170° circular visual field (calculated as $\tan\left(\frac{\alpha}{2}\right) = \frac{a}{2b}$, where α is the visual angle, a is the width of the screen and b is the distance from the eye to the screen). The projected obstacle varied in contrast, but maintained a width of 30° (measured in the middle of the visual field) and moved with a speed of $10^\circ\ \mathrm{s}^{-1}$ throughout all recordings (15 s). The perceived non-linearity of the size and movement of the visual stimulus by the LLE were not accounted for of two reasons: (i) The animals do not swim with constant speed or direction, so adjusting for non-linear movement seems counter-intuitive. (ii) Adjusting for the angular size of the moving bar would result in changes in overall light intensity of the projecting screen, which would affect the light ON/OFF response involved in detecting mangrove light shafts.[22,23] The movement direction of the obstacle (right-to-left or left-to-right) was determined by the micro-orientation of the LLE. Ideally, the eye was placed perpendicular to the projecting screen, but this was not always exact. In such cases, the bar was moved from the side to which the LLE was slightly turned. Though the bar moved from one side to the other, it remained within the visual field at all times to avoid changes in the overall intensity of the visual stimulus. The contrasts of the vertical bars were determined by uniformly illuminating the projection screen with the respective gray-tones, and measuring the irradiance (350 to 700 nm) using a USB-650 spectrometer fitted with a P400-2-VIS/NIR fiber (OceanOptics, Ostfildern, Germany). Irradiance was corrected for the absorption spectrum of the 500 nm *T. cystophora* opsin[49] present in the LLE.[45–47] Subsequently, the contrasts were calculated as for the behavioral experiments.

Treatment protocol

The visual stimulus consisted of three levels of the treatment factor called *Contrast* ($c = 0.20$, 0.40, and 0.80) to which the responding pacemaker signals were recorded (Figure S5). The total duration of each treatment sequence was 80 s, divided into three periods: 30 s stationary obstacle (pre-trial control), approx. 15 s visual stimulation of the LLE caused by the movement of the obstacle, concluding with 35 s stationary obstacle (post-trial control). The recording periods were spaced so that treatments were 2 min apart. The sequence of treatments was always tested from low to high contrast (i.e., $c = 0.2 \rightarrow c = 0.4 \rightarrow c = 0.8$), to avoid premature learning (no consequence when ignoring obstacle) (Figure S5B). Following the pre-training treatment sequence, the LLE was exposed to five consecutive treatments with the CS, using a $c = 0.20$ vertical contrast obstacle. The interval between treatments was 1 min. When the leading edge of the obstacle crossed the center of the visual field of the LLE, an electrical US was administered through the extracellular recording electrode (Figures 1D and S5). The US was a 50 ms square pulse of 100 mV and 100 nA (electrode resistance was approximately 1 MΩ when attached to the epidermal stalk nerve). The treatment protocol concluded with a second series of exposures to the three levels of contrast immediately after the US protocol, resulting in totally 11 exposures for each LLE. Three control protocols were followed: one in which the full protocol was completed but with a US of 0 mV, one in which the US was decoupled from the visual stimulus (CS), and one in which the CS and US were temporally uncoupled (unpaired). In the latter control experiment, the US was delivered with 60, 80, 70, 60, and 80 s delay in the five consecutive treatments respectively to avoid inducing trace conditioning. Each rhopalium was used for either the experimental series or for one of the control series. All protocols were completed within 1 h after detaching the rhopalium.

QUANTIFICATION AND STATISTICAL ANALYSIS

Analysis of behavioral data

The video recordings were converted into swim trajectories with a temporal resolution of 1 s using a custom-made program for MATLAB 2019a (MathWorks, Natick, MA, USA). The average distance to the closest wall and the swim speed was calculated from the trajectories, and the number of avoidance responses was counted manually. An avoidance response was defined as the medusa swimming towards the wall and then turning a minimum of 120° in two to three swim contractions with an increased pulse rate (see Garm et al. 2013[25] for supplementary video of this behavior). Additionally, the number of unsuccessful avoidances was counted manually. An unsuccessful avoidance was defined as a contact between the medusa's bell and the arena wall. When the medusa was swimming along the wall with continuous contact, it was regarded as one contact, not ending until both the bell and the tentacles were no longer in contact with the wall. Each trial of 7.5 min was divided into three periods of 2.5 min and the four behavioral parameters were compared between these three periods using PROC GLM in SAS (SAS OnDemand for Academics, SAS Institute 2020). Prior to the analysis, count data were square-root transformed in order to achieve normality and variance homogeneity. All four behavioral responses were analyzed simultaneously by including a manova statement in the GLM procedure. Each individual in an experiment was assigned a unique ID, which was treated as a random factor nested within treatments, and multiple observations on the same individuals were accounted for by means of a repeated measurements analysis. The full model included the factors *Treatment* (gray, black, uniform), *Period* (0–2.5, 2.5–5, 5–7.5 min) and the interaction between *Treatment* and *Period*. The effect of

Please cite this article in press as: Bielecki et al., Associative learning in the box jellyfish *Tripedalia cystophora*, Current Biology (2023), https://doi.org/10.1016/j.cub.2023.08.056

treatment was tested by means of an *F*-test using Mean Squares of individuals in the denominator. Since the manova revealed that there was an overall effect of treatment and time on the behavioral responses, and that *Treatment* and *Period* interacted, each treatment was analyzed separately with respect to how time affected the four response variables using repeated measurements analysis based on generalized estimating equations (GEE) (PROC GEE in SAS). The within-subject factor was ID of individuals, while *Period* was treated as a fixed factor. Post hoc comparisons were carried out by means of Tukey's Honestly Significant Difference (HSD) tests. p-values less than 0.05 were considered significant.

Analysis of neurophysiological data

We applied a three-parameter model to fit the observed time trends in spike frequencies during an experiment in order to investigate whether an OAB occurred. If the non-linear algorithm converged, the "Reaction" parameter (denoted y_m) predicts the maximum spike frequency during an OAB response, while the two shape parameters (*a* and *b*) determine the duration and location of the response (Figures S1–S4). An OAB response was deemed significant if (i) data were adequately described by the model ($p < 0.05$) and (ii) the estimated value of y_m was significantly ($p < 0.05$) larger than 0. However, to reduce the risk of type I errors, p-values were adjusted by means of the sequential Bonferroni procedure to obtain an experiment-wise error rate of 5% (Table 3).[32]

For a given experimental treatment and a given replicate, let t_i and t_{i+1} denote the time (in milliseconds) when two successive spikes occurred, so that the time interval between the two spikes becomes $\Delta t_i = t_{i+1} - t_i$, while the midpoint of the time interval between the two spikes can be found as $\bar{t}_i = (t_i + t_{i+1})/2$. The time intervals between successive spikes were converted to instantaneous frequencies given as $f_i = 1000/\Delta t_i$ Hz.

The standardized residual frequencies were calculated as the *n* differences between the observed frequency (f_i) during the *i*th time interval and the average frequency over the entire experiment ($\bar{f}$), i.e., $r_i = f_i - \bar{f}$, where $\bar{f} = \sum_{i=1}^{n} f_i/n$. Positive residual values indicate above average neural activity, which may simply be due to random variation in the number of spikes per time interval. However, a sequence of large positive residuals occurring after an eye has been subjected to a visual stimulus can be interpreted as an OAB response to the stimulus if the frequencies differ significantly from the background activity.

We model neural activity by means of the model

$$E(r_t) = \mu + \varphi(t) \qquad \text{(Equation 1)}$$

where $E(r_t)$ is the expected residual at time *t*. $\varphi(t)$ is the extra neural activity due to a stimulation (occurring at time $t = t_{stim}$) while μ is the mean activity during all time intervals where an eye does not show any response. Note that μ is equal to $\bar{r} = \sum_{t=1}^{n} r_t/n = 0$ if the stimulus does not elicit a response, otherwise μ will be negative.

The spike activity function φ (*t*) is modeled by the so-called SANDY function[50] given as

$$\varphi(t) = y_m C \left(\frac{t - T_1}{T_2 - T_1}\right)^a \left(\frac{T_2 - t}{T_2 - T_1}\right)^b (T1 \leq t \leq T2) \qquad \text{(Equation 2)}$$

where y_m is the maximum value of φ (*t*), while T_1 and T_2 are the values of *t* when an experiment starts and ends, respectively. *a* and *b* are two non-negative shape parameters that determine the location and duration of the spike activity function. *C* is a scaling constant ensuring that φ (*t*) is equal to y_m when the function peaks. It means that *C* is found as

$$C = \left(\frac{a}{a+b}\right)^{-a} \left(\frac{b}{a+b}\right)^{-b} \qquad \text{(Equation 3)}$$

The time at which φ (*t*) reaches its maximum (i.e., φ (*t*) = y_m) is found from

$$t_{peak} = \frac{aT_2 + bT_1}{a+b} \qquad \text{(Equation 4)}$$

In combination Equations 1 and 2 yield

$$E(r_t) = \mu + y_m C \left(\frac{t - T_1}{T_2 - T_1}\right)^a \left(\frac{T_2 - t}{T_2 - T_1}\right)^b \qquad \text{(Equation 5)}$$

Since eyes were not stimulated at exactly the same time, we replaced time *t* in the above equations with the adjusted time (t_{adj}), calculated as $t_{adj} = t - t_{stim}$. It means that $t_{adj} = 0$ at the time when the obstacle (the root mimic) commences to move across the screen, while T_1 and T_2 correspond to -30000 ms and 50000 ms, respectively, on the adjusted time axis.

We used PROC NLIN in SAS (SAS Institute 2020) to estimate the four parameters of Equation 5 (i.e., $p = 4$) as the values of μ, y_m, *a* and *b* that minimized the sum of squared differences between the observed (r_i) and predicted residuals ($E(r_i)$) at time $\bar{t}_i$, i.e.,

$$SS_{unexplained} = \sum_{i=1}^{N} (r_i - E(r_i))^2 \qquad \text{(Equation 6)}$$

N is the total number of observations (time intervals) available for each treatment, calculated as $N = \sum_{k=1}^{K} n_k$, where *K* is the number of replicates (eyes) per treatment, and n_k the number of time intervals for the k^{th} replicate.

Estimation of the model's parameters requires that the procedure converges towards a unique solution. If this was not achieved, it was interpreted as the activity function did not have a maximum, so that $E(r_i) = \mu = 0$. If the convergence criterion was met, the procedure yielded an F-value, calculated as F = MS(explained variation)/MS(unexplained variation), with p-1 = 3 df in the numerator and N-p-1df in the denominator. p-values less than 0.05 were considered as significant, implying that the model overall fitted the observed pattern in neural activity.

PROC NLIN also provides the asymptotic 95% confidence intervals for each parameter. If the interval for a given parameter did not include 0, the parameter was considered as significantly different from 0 at the 5% level. Alternatively, an approximate p-value for a given parameter (denoted β) can be obtained as $z = \widehat{\beta}/\mathrm{SE}(\widehat{\beta})$, where $\mathrm{SE}(\widehat{\beta})$ is the asymptotic standard error of $\widehat{\beta}$ and z is a standardized normally distributed variable.

We also used the estimated parameter values and their standard errors to plot the predicted response curve and its 95% confidence limits associated with a given treatment (Figures S1–S4), and to calculate t_{peak}. We were particularly interested in testing whether y_m was significantly larger than 0, because this demonstrates that the rhopalia showed a response to the treatment. However, to protect against false peaks, occurring by chance, we also required that the model provided a significant fit to data ($p < 0.05$). Furthermore, to protect against type I errors associated with multiple tests, we adjusted the significance level by applying a sequential Bonferroni procedure[32] to obtain an experimental-wise error rate of 5%.

In order to test whether the pre- and post-training phases within a given experimental set-up differed significantly, we replaced the parameters in Equation 5 with $\mu_B = \mu_A + \mu' x$, $y_{mB} = y_{mA} + y_m' x$, $a_B = a_A + a' x$ and $b_B = b_A + b' x$, where x is a dummy variable, which is 0 for series A (pre-training) and 1 for series B (post-training), so that $\mu' = \mu_B - \mu_A$, $y_m' = y_{mB} - y_{mA}$, $a' = a_B - a_A$ and $b' = b_B - b_A$. The model's eight parameters (μ_A, y_{mA}, a_A, b_A, μ', y_m', a' and b') were estimated simultaneously by fitting the model to the combined dataset of both series. The null hypothesis was that the two series were not statistically different (i.e., $\mu m' = y_m' = a' = b' = 0$). If the analysis of the full model revealed that both a' and b' were not significantly different from 0, it was interpreted as the two series were similar with respect to shape and location. We then reduced the model by omitting a' and b' from it and repeated the analysis to test for a difference between the two series with respect to OAB response, indicated by a significant value of y_m'. The fit of the reduced model was assessed by means of an F-test and the associated p-value. A significant p-value for model fit (based on the sequential Bonferroni procedure[32]) was used as criterion for whether the estimated value of y_m' was a reliable measure of the difference between the pre- and post-training phases. Finally, if y_m' was found to be significantly greater than 0, it was taken as an evidence of a training response.

In the 'unpaired CS + US' post-training phase, a significant reaction to contrast $c = 0.40$ was observed. This reaction, however, peaked significantly earlier ($t_{\mathrm{peak}} = 5.17$ s) than the average of the other significant reactions to the CS ($t_{\mathrm{peak}} = 6.34$ s) (see Table 3), and is more likely an artifact due to random variation in data (see Figure S4), rather than a true physiological reaction to the visual stimulus, stressing the importance of adjusting for multiple tests.[32] The underlying model (Equation 2) provided a significant fit to data in 11 out of the 24 treatment combinations (Table 3). The 11 values of t_{peak} obtained from these fits ranged from 5.17 s to 6.68 s. Based on these values, we calculated the average t_{peak} as 6.237 s with a standard error of 0.127 s. The 95% confidence limits for the mean value of t_{peak} were calculated by means of the t-distribution as $5.953 < t_{peak} < 6.521$ s. We suspect that the value of t_{peak} obtained from the unpaired, post-training treatment when $c = 0.40$ (i.e., $t_{peak} = 5.17$ s) is an outlier since the two-tailed probability of observing a deviation from the average t_{peak} equal to or larger than 1.067 s is $p = 7.862 \cdot 10^{-7}$. Consequently, if $t_{peak} = 5.17$ s is excluded from the calculations, the average value of t_{peak} becomes 6.344 s (95% CL: 6.170–6.518 s). Visual inspection of the graph (Figure S4) clearly shows that increased neural activity occurred over an extended period, starting some time before the visual stimulation. Furthermore, since t_{peak} was estimated by means of two parameters (a and b), both associated with relatively large standard errors, it seems likely that the point estimate of t_{peak} will be associated with considerable uncertainty, too.